Agricultural water allocation with climate change based on gray wolf optimization in semi-arid region of China

Zhidong Wang [1] , **Xining Zhao** [1, 2] , **Jinglei Wang** [Corresp., 3] , **Ni Song** [3] , **Qisheng Han** [Corresp. 3]

[1] College of Water Resources and Architectural Engineering, Northwest A & F University, Yangling, China

[2] Institute of Soil and Water Conservation, Northwest A&F University, 712100, Yangling, Shaanxi Province, China, Yangling, China

[3] Farmland Irrigation Research Institute of Chinese Academy of Agriculture Sciences/Key Laboratory of Crop Water Use and Regulation, Ministry of Agriculture and Rural affairs, Xinxiang, China

Corresponding Authors: Jinglei Wang, Qisheng Han
Email address: wangjinglei@caas.cn, hanqisheng@caas.cn

Background: We quantified and evaluated the allocation of soil and water resources in the Aksu River Basin to measure the consequences of climate change on an agricultural irrigation system. **Methods:** We first simulated future climate scenarios in the Aksu River Basin by using a statistical downscaling model (SDSM). We then formulated the optimal allocation scheme of agricultural water as a multiobjective optimization problem and obtained the Pareto optimal solution using the multi-objective grey wolf optimizer (MOGWO). Finally, optimal allocations of water and land resources in the basin at different times were obtained using an analytic hierarchy process (AHP). **Results:** (1) The SDSM is able to simulate future climate change scenarios in the Aksu River Basin. Evapotranspiration (ET_0) will increase significantly with variation as will the amount of available water albeit slightly. (2) To alleviate water pressure, the area of cropland should be reduced by 127.5 km^2 under RCP4.5 and 377.2 km^2 under RCP8.5 scenarios (3) To be sustainable, the allocation ratio of forest land and water body should increase to 39% of the total water resource in the Aksu River Basin by 2050.

Agricultural water allocation with climate change based on gray wolf optimization in a semi-arid region of China

Zhidong Wang [1,2], Xining Zhao[1,2], Jinglei Wang[3]*, Ni Song[3] and Qisheng Han[3]*

[1]College of Water Resources and Architectural Engineering, Northwest A & F University, Yangling 712100, China.

[2]Institute of Soil and Water Conservation, Northwest A&F University, 712100, Yangling, Shaanxi Province, China.

[3]Farmland Irrigation Research Institute of Chinese Academy of Agriculture Sciences/Key Laboratory of Crop Water Use and Regulation, Ministry of Agriculture and Rural affairs, Xinxiang, Henan 453003, China.

Corresponding Author:

Jinglei Wang;

Farmland Irrigation Research Institute of Chinese Academy of Agriculture Sciences/Key Laboratory of Crop Water Use and Regulation, Ministry of Agriculture and Rural affairs, Xinxiang, Henan 453003, China

Qisheng Han;

Farmland Irrigation Research Institute of Chinese Academy of Agriculture Sciences/Key Laboratory of Crop Water Use and Regulation, Ministry of Agriculture and Rural affairs, Xinxiang, Henan 453003, China

Email address:wangjinglei@caas.cn; hanqisheng@caas.cn

Abstract

Background: We quantified and evaluated the allocation of soil and water resources in the Aksu River Basin to measure the consequences of climate change on an agricultural irrigation system.

Methods: We first simulated future climate scenarios in the Aksu River Basin by using a statistical downscaling model (SDSM). We then formulated the optimal allocation scheme of agricultural water as a multiobjective optimization problem and obtained the Pareto optimal solution using the multi-objective grey wolf optimizer (MOGWO). Finally, optimal allocations of water and land resources in the basin at different times were obtained using an analytic hierarchy process (AHP).

Results: (1) The SDSM is able to simulate future climate change scenarios in the Aksu River Basin. Evapotranspiration (ET_0) will increase significantly with variation as will the amount of available water albeit slightly. (2) To alleviate water pressure, the area of cropland should be reduced by 127.5 km^2 under RCP4.5 and 377.2 km^2 under RCP8.5 scenarios (3) To be sustainable,

37 the allocation ratio of forest land and water body should increase to 39% of the total water resource

38 in the Aksu River Basin by 2050.

39

40 **Introduction**

41   Economic and social development are constrained by various factors, including shortages of

42 available water and land resources, climate change and environmental degredation. (Bai *et al.*,

43 2015). The IPCC's Sixth Assessment Report (AR6) has made clear that climate change is

44 intensifying the water cycle and affecting rainfall patterns (IPCC, 2021), which will have a

45 significant impact on the global hydrological cycle and water balance (Miller and Belton, 2014).

46 With rapid population and economic growth, it is difficult to recocile trade-offs among water and

47 land management, ecological environmental protection, and socio-economic development (Mei

48 *et al.*, 2010).

49   As the world population and consequent demand for food increase, safe water for

50 agricultural use has become increasingly scarce (Summerlin *et al.*, 2021). This phenomenon is

51 pronounced in arid and semiarid regions with irrigation (Rasouli *et al.*, 2012). The total amount

52 of argicultural irrigation is often determind by planting area and planting structure. However, ET

53 is usually calculated using a crop coefficient in irrigation planning with evapotranspiration (ET_0)

54 as a key indicator (Wu *et al.*, 2021).

55   Recent studies have found that ET_0 should change with the effects of climate change,

56 especially where agricultural water consumption accounts for a large proportion of use (Zou *et*

57 *al.*, 2020). The ability to accurately simulate future climatic scenaros will be the basis for

58 estimating the ET_0. Although future climate conditions can be roughly estimated using general

59 circulation models (GCMs), meeting requirements for high resolution has been challenging

60 (Wilby *et al.*, 2002). Therefore, it is necessary to use downscaling methods to "shrink" the study

61 area to specific areas or sites for practical application (Hewitson and Crane, 2006).

62   There are two dominant downscaling approaches: dynamic and statistical. Statistical

63 downscaling is widely used because of its simple operation and low cost (Vallam and Qin,

64 2018). A statistical downscaling model (SDSM) is used to produce the required high-resolution

65 climate projection by developing a statistical relationship between the large- and local-scale

66 climate variables (Gebrechorkos *et al.*, 2019). As such it is more stuitable for climate change

67 simulation at local scales. However, in previous studies, the impact of climate change on

68 regional inflow and demand and the feedback relationship between supply and demand were

69 ignored (Fu et al., 2014). For example, Sun et al. (2018) have considered the impact of climate

70 change on watershed runoff, but ignored the impact of different climatic conditions on

71 agricultural and ecological water demand. Therefore, how to simultaneously consider changes in

72 water resources and water demand under climate change and realize a balanced allocation of

73 regional water and land resources is a problem that needs to be solved urgently.

74   However, industrial / domestic and ecological water are considered equally important for

75 regional development. Water and land optimization allocation is also a complex problem that

76 involves many elements (Habibi *et al.*, 2016). How to rationalize planting structure with the

77 effects of climate change is an important consideration in water resource management. The best

78 way to solve this problem is to build a multi-objective model for optimization. Approaches such

79 as evolutionary (EA), genetic (GA), and nondominated sorting genetic algorithms (NSGA-II),

80 linear (LP) and non-linear programming (NLP), among others, have been applied to optimize

81 water and land resources (Keshtkar *et al.*, 2020). These methods provide multiple options for

82 decision makers by finding a model Pareto solution set. However, most have a number of

83 shortcomings, (e.g., local optima traps or slow convergence). The grey wolf optimizer (GWO)

84 algorithm, which was proposed by Mirjalili et *al.* (2014), is a relatively novel population-based

85 metaheuristic algorithm that combines fast convergence and high optimization accuracy Rashidi

86 *et al.*, 2018). The GWO algorithm utilizes the simulated social leadership and encircling

87 mechanism in order to find the optimal solution for single-objective optimization problems

88 (Mirjalili et *al.*, 2014). For preforming multi-objective optimization, the multi-objective GWO

89 (MOGWO) extends the advantages of GWO to more complex scenarios. However, the

90 shortcomings of GWO (initial value effects, local optimum traps) when solving multi-objective

91 problems have been improved (Mirjalili et *al.*, 2016).

92   Xinjiang province is typical of arid and semi-arid regions in China that lack

93 significant water resources that are primarily generated by glacier meltwater in adjacent

94 mountains (Chen *et al.*, 2020). Water shortages have become a source of conflict in the Tarim

95 River Basin of Southern Xinjiang with intense confrontations between environmental protection

96 and economic development (Lam *et al.*, 2011). As an ecologically fragile area, the Tarim River

97 Basin has experienced a significant decline of its riparian desert forests (Zhang *et al.*, 2019).

98 Additionally, the Tarim River Basin is a major source of cotton and fruit production. Therefore,

99   it is particularly important to improve water use efficiency and optimize allocation of water

100 resources in this region.

101   To help decision makers formulate regional resource allocation strategies in future climate

102 change scenarios, we developed a multi-objective water and soil resource allocation model based

103 on MOGWO and AHP. The main contributions of our model lie in the following aspects: (1)

104 forecast regional climate change scenarios using the SDSM model; (2) calculate regional water

105 supply and demand in different climate scenarios; (3) determine water consumption among crops

106 and establish a multi-objective programming model using the MOGWO algorithm to solve

107 water-use conflicts for agricultural production, ecosystems, and drinking water supply; (4) select

108 the most suitable options from the Pareto solutions using an analytic hierarchy process (AHP).

109

Materials & Methods
110

Study area
111

112   The study area was the Aksu Valley (75° 35′ − 82° 00′ E, 40° 00′ − 42° 27′ N,

113 excluding Akqi) in Xinjiang, China. The area is approximately $3.6 \times 10^4 \, \mathrm{km}^2$, including 6

114 counties or cities in the Aksu area (Aksu, Wensu, Awati, Wushi, Keping and Alar). It is served

115 by the western upper reaches of the Tarim River Basin (**Error! Reference source not found.**)

116 and sand dunes are the predominant landform (El-Tantawi *et al.*, 2019). The water used for

117 agricultural irrigation makes up more than 95% of the total regional water consumption. The

118 most important irrigated crop is cotton, which has increased in annual planting area (Li *et al.*,

119 2020).

Data Sources
120

121   Meteorological data were obtained from the China Meteorological Science Data Network

122 (1961–2005) (http://data.cma.cn/). Large-scale climate variables (predictors) for the current

123 climate and future scenarios under the RCPs in years 1961 to 2050 obtained from Canadian

124 Climate Data and Scenarios (http://climate-scenarios.canada.ca/). We used grid resolution 2.815°

125 latitude by 2.815° longitude. River discharge data (1961–2005) were from the Aksu Valley

126 Chronicles (Aksu River Basin Management Office, 2006). Socio-economic data were gathered

127 from the Aksu Region Yearbook and Xinjiang Construction Corps Yearbook (Bureau of

128 Statistics of Xinjiang Production and Construction Corps, 2009).

Simulation of climate scenarios
129

130 Statistical downscaling model under two scenarios (RCP 4.5 and RCP 8.5)

131   RCP 2.6 represents a stringent mitigation scenario, RCPs 4.5 is intermediate mitigation

132   scenarios and RCP 8.5 is low mitigation scenario with very high greenhouse emissions (Carvalho

133   et al., 2019). Due to better representation of actual emissions since 2000 by other RCPs (Peters et

134   al., 2012), we excluded RCP 2.6 in this study. The CanESM2 predicators provide 26 parameters

135   (https://climate-scenarios.canada.ca/?page=pred-canesm2). To produce climate data for future

136   analyses, the SDSM model was parameterized by inputting daily observations (**Fig. 1**) and 26

137   predictors from CanESM2 (1961–1990 data for model building and 1991–2005 data for the

138   model validation). Five predictors (daily maximum and minimum temperature, daily relative

139   humidity, annual rainfall, and annual sunlight) were selected based on the correlation matrix,

140   partial correlation, and P-value (Fowler *et al.*, 2007) (**Supplementary Table 1**). Final model

141   accuracy was examined using both the coefficient of determination (R^2) and Root Mean Square

142   Error (RMSE) (Wood *et al.*, 2004) (**Supplementary Table 1**).

143   **Estimation of water demand and supply in Aksu River basin**

144   (1) Total water demand

145   a.   Agricultural water demand

146   The Hargreaves equation and downscaling simulation results were used to calculate the

147   reference crop evapotranspiration (ET_0). Previous research showed that Hargreaves equation had

148   good applicability in arid and semi-arid regions (Wang, et al., 2013)

$$ET_0 = \frac{K}{\lambda}(T_{max} + T_{min})^n \cdot (T_{mean} + T_{off}) \cdot R_a \qquad (1)$$

$$T_{mean} = (T_{max} + T_{min})/2 \qquad (2)$$

151   Where K is the conversion coefficient (recommended value=0.0023), λ is the latent heat of water

152   vaporization (recommended value=2.45 MJ/kg), T_{max}, T_{min} are the highest and lowest

153   temperature (°C), n is the exponential coefficient (recommended value=0.5), T_{mean} is the average

154   temperature (°C), T_{off} is the temperature constant (recommended value=17.8), and R_a is the solar

155   insolation at the top of the atmosphere $MJ/(m^2/d)$(Bautista, *et al.*, 2009). The water requirement

156   of the main crops in the study area was calculated as:

$$W_{GD} = \sum_{i=1}^{n}\sum_{j=1}^{m} P_i(ET_{0ij}K_{cij} - 0.52T_{ij}) \qquad (3)$$

158   where W_{GD} is the water requirement per unit area of arable land ($10^4 m^3/km^2$), P_i is the proportion

159   of crop i per unit area of arable land, ET_{0ij} is the reference crop water requirement for crop i in

160 month j (growing season), K_{cij} is month j (growing season) of crop i, T_{ij} is month j (growing

161 season) of crop i rainfall, and 0.52 is the rainfall utilization coefficient (Rahman *et al.*, 2008).

162 Irrigation water requirement per unit area:

$$W_{GDi} = W_{GD} * a_i/b_{i1} + W_{GD} * (1 - a_i)/b_{i2} \tag{4}$$

164 where W_{GDi} is the amount of irrigation water per unit of arable land, a_i is the proportion of water-

165 saving irrigation area in year i, and b_{i1} and b_{i2} are respectively the conventional and water-saving

166 irrigation water utilization coefficients in year i.

167 b. Industrial and domestic water demand (W_{IDi})

168 According to 2018 statistics data, industrial water consumption per km^2 was calculated by

169 dividing the total industrial outputs with total industrial water consumption in Aksu. The water

170 consumption of the industrial added value of ten-thousand yuan was approximately 110 m^3.

171 Residential water consumption per unit area is calculated using the resident population and the

172 water consumption per municipality. According to the Plan for Reform and Development of the

173 Aksu Region (2020-2050), and these are summed for the Aksu River Basin (**Table 1**).

174 c. Ecological water demand

175 We consider water for the forests and water bodies as ecological. The formula for the calculation

176 of forest demand is:

$$W_{LD} = K_s\sum\nolimits_{j=1}^{m}(ET_{0j}K_{cj} - 0.52T_j) \tag{5}$$

178 where W_{LD} is the water demand per unit area of woodland in the watershed ($10^4 m^3/km^2$), K_s is

179 the soil moisture limitation coefficient, ET_{0j} is month j of the forest land (growing season)

180 reference crop water demand, K_{cj} is the crop coefficient of forest land in month j, and T_j is the

181 rainfall of forest land in month j.

$$W_{LDi} = W_{LD}/b_{i2} \tag{6}$$

183 Here, W_{LDi} is the amount of irrigation water per unit of woodland, and b_{i2} is the water-saving

184 irrigation water utilization coefficient in decade i.

185 The water demand for the water bodies:

$$W_{WA} = 0.58 * E_0 \tag{7}$$

$$ET_0 = 0.556 * E_0 \tag{8}$$

188 where W_{WA} is water demand per unit of water area. Xi and Cheng (2002) estimated the

189 conversion coefficient between a 20 cm^2 dish and a 20 m^2 evaporating pool was 0.58. ET_0 was

190   estimated by multiplying E_0 by a coefficient 0.556 (Xi and Cheng, 2002). We assume that

191   grasslands are not irrigated in this study.

192   **Total water demand = total agricultural water deman**d + **total industrial and domestic**

193   **water demand + total ecological water demand**

194   (2) Total water supply in the future climate

195   **Total water supply = available surface water + available groundwater resources**

196   The sum of river flow of two hydrological stations (Sahliguilanke and Xiehela) was used as

197   water resource input and the river flow at the Alar station was used as the residual amount of

198   water resource (**Fig. 1**). The difference between the two flows was computed as **the amount of**

199   **available surface water** in the study basin. A neural networks model was used to estimate

200   runoff data for the hydrometric station.

201   The specific analysis we used followed Zarghami *et al*. (2011). Using the runoff and

202   meteorological data from 1958–1995, the feedforward neural network models between runoff

203   and meteorological factors were parameterized. Data from 1996–2003 were selected for

204   verification and the fluctuation and precision judgment indices were set to evaluate neural

205   network performance. Because the number of network layers was 20, the two indexes reach the

206   minimum value by trial-and-error. The following data were used in the models: runoff (R),

207   precipitation (P), relative water content (RWC), minimum temperature (T_{min}), maximum

208   temperature (T_{max}), average daily sunshine hours (ADS), mean temperature (T_{mean}) and ET_0, all

209   indexed to time (years). The resulting model is:

210          $$R(t)=f(P(t), RWC(t), T_{max}(t), T_{min}(t), T_{mean}(t)ADS(t)ET_0(t)) \qquad (9)$$

211   The modeling process was performed using the ANN toolbox in the MATLAB environment.

212   Annual average meteorological values predicted by SDSM under RCP4.5 and RCP8.5 scenarios

213   were entered into the neural network model to estimate the annual runoff at the hydrological

214   station. Finally, an expected future amount of water resources could be calculated from the

215   estimated hydrological station data. The **available amount of groundwater** in Aksu River Basin

216   was considered as unchanged.

217   **Multi-objective optimal allocation model of water and soil resources**

218   The multi-objective optimal allocation model must cover the balance of the economic, social

219   and ecological benefits. We used the gross national product (GDP) as the economic indicator, the

220 maximum benefit of water per cubic meter as the social indicator and ecological green equivalent

221 as the ecological indicator. The computational formula is:

222
$$F_1(X) = \max \sum_{i=1}^{n} \sum_{j=1}^{m} a_{ij} X_{ij} \tag{10}$$

223
$$F_2(X) = \max \frac{\sum_{i=1}^{n} \sum_{j=1}^{m} a_{ij} X_{ij}}{\sum_{i=1}^{n} \sum_{j=1}^{m} b_{ij} X_{ij}} \tag{11}$$

224
$$F_3(X) = \max \sum_{i=1}^{n} \sum_{j=1}^{m} c_{ij} X_{ij} \tag{12}$$

225
$$\sum_{i=1}^{n} b_{ij} X_{ij} \leq W_s \tag{13}$$

226
$$\sum_{i=1}^{n} X_{ij} = T \tag{14}$$

227
$$\sum_{j=1}^{n} X_{1j} \geq PL_{min} \tag{15}$$

228
$$\sum_{j=1}^{n} X_{2j} \geq FL_{now} \tag{16}$$

229
$$\sum_{j=1}^{n} X_{3j} \geq CL_{now} \tag{17}$$

230
$$\sum_{j=1}^{n} X_{4j} \geq WL_{now} \tag{18}$$

231
$$\sum_{j=1}^{n} X_{5j} = NL_{now} \tag{19}$$

232 where $F_1(X)$ is total GDP, $F_2(X)$ is the utilization of maximum benefits per cubic meter of water,

233 $F_3(X)$ is the ecological green equivalent of the river basin, X_{ij} is the area of land types in each

234 area (km^2), a_i is gross national product per unit area of each land type (10,000 yuan/km^2), b_i is the

235 water demand per unit area of each land use type (m^3), and c_i is the green equivalent value of

236 each area of each land type. T is the total area (km^2), PL_{min} is the red line of cultivated land in the

237 study area (km^2), FL_{now} is the current forest area (km^2), BL_{now} is the current construction land

238 area, WL_{now} is the current water area, and NL_{now} is the current unused land area.

239 **The MOGWO algorithm and the optimal solution**

240 **(1)** Design of MOGWO algorithm

241 We modified the grey wolf algorithm (GWO) to incorporate two new components (storing

242 non-dominated Pareto optimal solutions archive and a leader selection strategy) to comprise the

243 MOGWO (Mirjalili *et al.*, 2016). The detailed procedures are described in **Fig. 2**.

244 We obtained a set of non-dominated solutions for the multi-objective model. The parameter

245 settings were number of wolves=100, achieve=100, range=20% and iterations=100.

246 **(2)** The best optimal value for multi-objective model based on analytic hierarchy process method

247 (AHP)

248   The AHP is introduced to transform the process into hierarchical problems. To establish a

249   judgment matrix, the relative weight of each target is determined. At the same time, the

250   consistency index of the judgment matrix is calculated to verify the validity of the weight. The

251   consistency of the matrix is considered acceptable when the consistency ratio (CR) is less than

252   0.1. We determined importance indicators for establishing the judgment matrix (**Table 2**) and the

253   proportions and test indicators of the three planning goals calculated by the analytic hierarchy

254   process (**Table 3**).

Results

Projected future climate and water resource change

257   We projected temperatures and precipitation at the Aksu Basin using the downscaled global

258   climate models (GCMs) (**Fig. 3**). Warming was predicted for this area's subregions. By the year

259   2050 (starting in 2020), the projected temperature could increase up to 1.3, 0.9, 0.8, and 0.2 °C,

260   at Aksu, Keping, Alar, and Akqi under RCP4.5, respectively. Under the RCP8.5 climate

261   scenarios, the temperatures were predicted to increase at a faster rate. As opposed to temperature

262   trends, the precipitation showed decreasing trends except at the Keping station.

263   The minimum and maximum temperatures predicted by SDSM from 2006 to 2050 change

264   over the whole basin's ET_0 (**Fig. 4, Fig. 5**). ET_0 values of the four weather stations showed an

265   upward trend during the period 2010–2050. There was no significant difference between the

266   RCP4.5 and RCP8.5 climate scenarios during the first years, but ET_0 has an increasingly higher

267   value under RCP8.5 scenarios relative to RCP4.5 after 2035. The difference value is expected to

268   be as high as 50 mm by 2050.

269   By using the neural network model to estimate the runoff flow of the hydrological station, the

270   available surface water in the basin gives a trend of slow future increase **(Fig. 6).** Until 2050, the

271   annual average runoff is predicted to increase $7.963 \times 10^8 \, m^3$ and $10.41 \times 10^8 \, m^3$ under RCP4.5

272   and RCP8.5, respectively. The amount of runoff was higher under the RCP8.5 scenario than the

273   RCP4.5 scenario **(Table 4)**.

The optimal allocation of the water and land resources

275   Future water shortage is predicted to be about $5.83 \times 10^8 m^3$ in the basin (**Table 5**). The

276   Pareto frontier under the five scenarios obtained by MOGWO is shown in **Supplementary Fig.**

277   **1**; the specific values of water and soil resource allocation in the basin are shown in

278   **Supplementary Table 2-7**. Due to the high emission concentration (RCP8.5), with the exception

279   of construction land, the water demand per unit area of the other land types is higher compared to

280   the low emission concentration (RCP4.5). Although the total cultivated area in the basin under

281   the two climate scenarios is similar, the change of cultivation in each region of the basin differs.

282   Water and land resource allocation in the Recent-term (2020), medium-term (2035), and long-

283   term (2050) plan under two emission concentrations show, in general, a trend of decreasing

284   arable land and grassland and increasing other land (**Fig. 7**). The arable land areas of Awati,

285   Aksu, and Alar exhibited a continuous downward trend as the result of the policy for restoring

286   farmland to save water, but the arable land areas is likely to continue to increase in Wushi

287   County (**Fig. 8**). In addition, the area of grassland in the Wushi and Wensu regions is trending

288   downward, while the Alar is increasing (**Fig. 9**).

289

290   **Discussion**

291

292   We found that SDSM had higher predictive accuracy for temperature relative to rainfall

293   using a formal accuracy index. This may mimic the model's limitations in simulating rainfall

294   (Wilby et al., 2002). Downscaled climate change model scenarios suggest that the warm-wet

295   climate trend will continue in the semi-arid region. Rainfall shows a declining trend (except for

296   Keping station) in the region during 2021–2050, which has been also found in other studies

297   (Chu *et al*., 2010; Wilby and Dawson, 2013; Zhu *et al*., 2019).

298   The change of ET_0 caused by climate change will have a significant impact on agricultural

299   and ecological water demand (Guo and Shen, 2016; Hadinia *et al*., 2016). ET_0 values in the Aksu

300   River basin trend upward in the future (Figure 6) as in other areas of China such as the Tibetan

301   Plateau, Haihe River Basin and Hetao Irrigation District (Wang *et al*., 2013; Xing *et al*., 2014;

302   Zhou *et al*., 2017). The increasing ET_0 rate was also inversely related to elevation (Zou *et al*.,

303   2020), therefore ET_0 of the Akqi station had the lowest increasing rate in Aksu River basin.

304   Because of the hydrology of Xinjiang under future climate change scenarios (Li *et al*., 2020;

305   Shen *et al*., 2020; Xu *et al*., 2010), we suggest that surface runoff in the basin will trend upward

306   in the future. We suspect that the main reason for increased runoff will be an increase in

307   temperature leading to amplified loss of seasonal snow cover, glacier and ice sheet melting

308   (IPCC, 2021). In the past 30 years, ice and snow melt water has been increasing and will

309   continue to increase until 2050 in the Aksu River Basin (Wang, 2018; Zhang, 2010), which also

310   supports our model results. Ding and Reng (2007) reported that glacier melt water around the

311 Tarim Basin would continually grow potentially reaching a level of 10^8 m³/a (Xia Jun, 2011).

312 The upward trend in runoff is also predicted to be greater under RCP 8.5 than RCP4.5 (**Fig. 6**).

313   Water scarcity continues to be a major crisis in the Aksu River Basin. With the ET_0 increase

314 water demand from agricultural production and ecological protection has increased annually. The

315 multi-objective allocation of soil and water resources to economic, societal, and ecological goals,

316 compel us to recommend reducing the area of cultivated land to alleviate the current water

317 shortage (Xu *et al.*, 2010). Currently, the Aksu River Basin is facing a shortage of water

318 resources estimated to be 5.83×10^8 m³ (**Table 5**). To balance water supply and demand, the

319 Aksu River Basin needs to reduce agricultural water use as a measure to protect the environment.

320 The most effective mitigation action is to reduce the arable land area. Forests and water bodies

321 should be expanded to strengthen ecological protection and improve ecosystem services.

322 Therefore, regions should adopt alternative allocation strategies to achieve the optimal

323 comprehensive benefits for the whole basin. Decision makers should enact recommended

324 configurations according to their own conditions under a changing climate and in different

325 regions.

326   Notably, the change of cultivation in each region of the basin differs. The arable land areas

327 of Awati, Aksu, and Alar exhibited a continuous downward trend as the result of the policy for

328 restoring farmland to save water, but the arable land areas is likely to continue to increase in

329 Wushi County (**Fig. 8**). The cause of this heterogeneity may be the different water requirements

330 per unit area of arable land in each county under the two scenarios. The output value per unit

331 area of Wushi County is lower than other regions due to the large proportion of crops planted on

332 arable land. As well, water demand per unit area is smaller than in other regions. If water

333 shortages constrain watershed development and are red line constraint of arable land, then lower

334 water use in Wushi will have a greater impact on the overall benefits of the entire watershed than

335 a low output value. We provide the following policy recommendations: To cope with this

336 shortage in the basin and measure including strictly following the "red line" restriction of

337 cultivated land, the area of the cropland should be reduced by 127.5 km² under RCP4.5 or 377.2

338 km² under RCP8.5 models. For the sake of ecological sustainability, the allocation ratio of forest

339 and water bodies should increase to 39% of the total water volume in the Aksu River Basin by

340 2050.

341   There is some limitation in this study, and the model could still be improved. For example,

342   due to the lack of data on future the cultivated land planting structure, we used current cultivated

343   planting structure for calculating future water demand per unit area. And in the AHP method, the

344   interconnection between the factors in the criterion level was ignored and considered as

345   independent of each other, and the factors could be refined in the later study to make the results

346   closer to the actual situation.

347

Conclusions

349   In the future, the ET_0 of the Aksu River Basin will increase variably according to climate

350   predictions of an SDSM model. Our study indicated that the water resources, mainly generated

351   by glacier/snow meltwater, increased according to the neural network model. Climate change

352   may have beneficial effects on agriculture in Aksu River Basin. This outcome may force

353   governments to find new and sustainable adaptation strategies to rescue the future water supply.

354   The water governance in this region should be more flexible and decentralized to cope with

355   climate change.

356

Acknowledgements

358   We are very thankful to Dr. John Wilmshurst for carefully reading and polishing the manuscript.

359

References

361   Aksu River Basin Management Office (2006) *Aksu valley chronicles*, Beijing, China, Fangzhi Press.

362   Bai, T., Chang, J., Chang, F.-J., Huang, Q., Wang, Y., and Chen, G. (2015) Synergistic gains from the multi-

363   objective optimal operation of cascade reservoirs in the Upper Yellow River basin. Journal of Hydrology, **523**,

364   758–767.

365   Bautista, F., Bautista, D., Delgadocarranza C. (2009) Calibration of the equations of Hargreaves and

366   Thornthwaite to estimate the potential evapotranspiration in semi-arid and subhumid tropical climates for

367   regional applications. *Atmósfera*, 22(4): 331-348.

368   Bureau of Statistics of Xinjiang Production and Construction Corps (2009) *Statistical Yearbook of Xinjiang*

369   *Production and Construction Corps.*, Beijing, China, NBS.

370   Carvalho, JS., Graham, B., Rebelo, H., Bocksberger, G., Meyer, CFJ., Wich S., Kühl, HS. (2019) A global risk

371   assessment of primates under climate and land use/cover scenarios. Global Change Biology 25:3163–3178.

372   DOI: 10.1111/gcb.14671.

373   Chen, W., Ding, J., Wang, J., Zhang, J., and Zhang, Z. (2020) Temporal and spatial variability in snow cover

374   over the Xinjiang Uygur Autonomous Region, China, from 2001 to 2015. PeerJ, **8**, e8861.

375   Chu, J. T., Xia, J., Xu, C.-Y., and Singh, V. P. (2010) Statistical downscaling of daily mean temperature, pan
376   evaporation and precipitation for climate change scenarios in Haihe River, China. Theoretical and Applied
377   Climatology, **99**(1), 149–161.
378   Ding, Y. H. and Reng, G. Y. (2007) *Climate Change National Assessment Report,* Beijing, China, Science
379   Press.
380   El-Tantawi, A. M., Bao, A., Chang, C., and Liu, Y. (2019) Monitoring and predicting land use/cover changes
381   in the Aksu-Tarim River Basin, Xinjiang-China (1990–2030). Environmental Monitoring and Assessment, **191**
382   (8), 480.
383   Fowler, H. J., Blenkinsop, S., and Tebaldi, C. (2007) Linking climate change modelling to impacts studies:
384   recent advances in downscaling techniques for hydrological modelling. International Journal of Climatology,
385   **27**(12), 1547–1578.
386   Frenken, K. and Gillet, V. (2012) Irrigation water requirement and water withdrawal by country. FAO, Rome,
387   Italy.
388   Fu, Y H., Guo, P., Fang, S Q., Li, M. (2014) Optimal water resources planning based on interval-parameter two-
389   stage stochastic programming. *Trans. CSAE*, **30**:73-81.
390   Gebrechorkos, S. H., Hülsmann, S., and Bernhofer, C. (2019) Statistically downscaled climate dataset for East
391   Africa. Scientific Data, **6**, 31.
392   Guo, Y. and Shen, Y. (2016) Agricultural water supply/demand changes under projected future climate change
393   in the arid region of northwestern China. Journal of Hydrology, **540**, 257–273.
394   Habibi Davijani, M., Banihabib, M. E., Nadjafzadeh Anvar, A., and Hashemi, S. R. (2016) Optimization
395   model for the allocation of water resources based on the maximization of employment in the agriculture and
396   industry sectors. Journal of Hydrology, **533**, 430–438.
397   Hadinia, H., Pirmoradian, N., and Ashrafzadeh, A. (2016) Effect of changing climate on rice water
398   requirement in Guilan, north of Iran. Journal of Water and Climate Change, **8**(1), 177–190.
399   Hewitson, B. C. and Crane, R. G. (2006) Consensus between GCM climate change projections with empirical
400   downscaling: precipitation downscaling over South Africa. International Journal of Climatology, **26**(10),
401   1315–1337.
402   IPCC (2021) Climate change widespread, rapid, and intensifying – IPCC — IPCC. [online]
403   https://www.ipcc.ch/2021/08/09/ar6-wg1-20210809-pr/ (Accessed December 24, 2021).
404   Keshtkar, H., Bozorg-Haddad, O., Fallah-Mehdipour, E., and Loáiciga, H. A. (2020) Groundwater safe yield
405   powered by clean wind energy. Environmental Monitoring and Assessment, **192** (7), 419.
406   Lam, T. Y., Kleinn, C., and Coenradie, B. (2011) Double sampling for stratification for the monitoring of
407   sparse tree populations: the example of Populus euphratica Oliv. forests at the lower reaches of Tarim River,
408   Southern Xinjiang, China. Environmental Monitoring and Assessment, **175** (1–4), 45–61.
409   Li, Y., Wang, H., Chen, Y., Deng, M., Li, Q., Wufu, A., Wang, D., and Ma, L. (2020) Estimation of regional
410   irrigation water requirements and water balance in Xinjiang, China during 1995–2017. PeerJ, **8**, e8243.
411   Li, Z., Shi, X., Tang, Q., Zhang, Y., Gao, H., Pan, X., Déry, S. J., and Zhou, P. (2020) Partitioning the
412   contributions of glacier melt and precipitation to the 1971–2010 runoff increases in a headwater basin of the
413   Tarim River. Journal of Hydrology, **583**, 124579.
414   Mei, H., Liuyuan, Duhuan, and Yangxiaoyan (2010) Advances in Study on Water Resources Carrying
415   Capacity in China. Procedia Environmental Sciences, **2**, 1894–1903.
416   Miller, K. A. and Belton, V. (2014) Water resource management and climate change adaptation: a holistic and
417   multiple criteria perspective. Mitigation and Adaptation Strategies for Global Change, **19**(3), 289–308.
418   Mirjalili, S., Mirjalili, S. M., Lewis, A. (2014) Grey wolf optimizer. Advances in Engineering Software, 69,
419   46–61.

420 Mirjalili, S., Saremi, S., Mirjalili, S. M., and Coelho, L. dos S. (2016) Multi-objective grey wolf optimizer: A
421 novel algorithm for multi-criterion optimization. Expert Systems with Applications, **47**, 106–119.
422 Peters, GP., Marland, G., Le, Quéré C., Boden, T., Canadell, JG., Raupach, MR. (2012) Rapid growth in CO2
423 emissions after the 2008–2009 global financial crisis. Nature Climate Change 2:2–4. DOI:
424 10.1038/nclimate1332.
425 Rahman, M. M., Islam, M. O., and Hasanuzzaman, M. (2008) Study of Effective Rainfall for Irrigated
426 Agriculture in South-Eastern Part of Bangladesh. World Journal of Agricultural Sciences, **4**(4), 453–457.
427 Rashidi, K., Mirjalili, S. M., Taleb, H., and Fathi, D. (2018) Optimal Design of Large Mode Area Photonic
428 Crystal Fibers Using a Multiobjective Gray Wolf Optimization Technique. Journal of Lightwave Technology,
429 **36**(23), 5626–5632.
430 Rasouli, F., Kiani Pouya, A., and Cheraghi, S. A. M. (2012) Hydrogeochemistry and water quality assessment
431 of the Kor-Sivand Basin, Fars province, Iran. Environmental Monitoring and Assessment, **184** (8), 4861–4877.
432 Shen, Y.-J., Shen, Y., Guo, Y., Zhang, Y., Pei, H., and Brenning, A. (2020) Review of historical and projected
433 future climatic and hydrological changes in mountainous semiarid Xinjiang (northwestern China), central Asia.
434 CATENA, **187**, 104343.
435 Summerlin, H. N., Pola, C. C., McLamore, E. S., Gentry, T., Karthikeyan, R., and Gomes, C. L. (2021)
436 Prevalence of Escherichia coli and Antibiotic-Resistant Bacteria During Fresh Produce Production (Romaine
437 Lettuce) Using Municipal Wastewater Effluents. Frontiers in Microbiology, **12**, 660047.
438 Sun, J., Li, Y P., Zhuang, X W., Jin, S W., Huang, G H., Feng, R F. (2018) Identifying water resources management
439 strategies in adaptation to climate change under uncertainty. *Mitig Adapt Strat Gl*, *23*,553-578.
440 Vallam, P. and Qin, X. S. (2018) Projecting future precipitation and temperature at sites with diverse climate
441 through multiple statistical downscaling schemes. Theoretical and Applied Climatology, **134** (1), 669–688.
442 Wang, C. (2018) An integrated approach for modeling the climate-driven streamflow in the typical basins in
443 the Southern slopes of Tianshan Mountains based on downscaling the earth data products.
444 Wang, W., Xing, W., Shao, Q., Yu, Z., Peng, S., Yang, T., Yong, B., Taylor, J., and Singh, V. P. (2013)
445 Changes in reference evapotranspiration across the Tibetan Plateau: Observations and future projections based
446 on statistical downscaling. Journal of Geophysical Research: Atmospheres, **118** (10), 4049–4068.
447 Wang, Y., Li, S., Xu, X., Lei, J., Jin, X., Wang, Q., Zhang, Z. (2013) Applicability of Hargreaves method in
448 estimating reference evapotranspiration in Taklamakan Desert Hinterland. Journal of Desert Research, 33(2),
449 367-372.
450 Wilby, R. L. and Dawson, C. W. (2013) The Statistical DownScaling Model: insights from one decade of
451 application. International Journal of Climatology, **33**(7), 1707–1719.
452 Wilby, R. L., Dawson, C. W., and Barrow, E. M. (2002) sdsm — a decision support tool for the assessment of
453 regional climate change impacts. Environmental Modelling & Software, **17**(2), 145–157.
454 Wood, A. W., Leung, L. R., Sridhar, V., and Lettenmaier, D. P. (2004) Hydrologic Implications of Dynamical
455 and Statistical Approaches to Downscaling Climate Model Outputs. Climatic Change, **62**(1), 189–216.
456 Wu, H., Xu, M., Peng, Z., and Chen, X. (2021) Temporal variations in reference evapotranspiration in the
457 Tarim River Basin, Central Asia. PLoS ONE, **16**(6). [online]
458 https://www.ncbi.nlm.nih.gov/pmc/articles/PMC8208581/ (Accessed August 11, 2021).
459 Xi, Y. Y. and Cheng G C (2002) Calculate the evaporation of the reservoir surface from the 20cm evaporation
460 pan data and wind speed. Hydropower station design, (2), 76–78.
461 Xia Jun, L. C. (2011) Opportunity and Challenge of the Climate Change Impact on the Water Resource of
462 China. Advances In Earth Science, **26**(1), 1–12.
463 Xing, W., Wang, W., Shao, Q., Peng, S., Yu, Z., Yong, B., and Taylor, J. (2014) Changes of reference
464 evapotranspiration in the Haihe River Basin: Present observations and future projection from climatic variables
465 through multi-model ensemble. Global and Planetary Change, **115**, 1–15.

466   Xu, C., Chen, Y., Yang, Y., Hao, X., and Shen, Y. (2010) Hydrology and water resources variation and its
467   response to regional climate change in Xinjiang. Journal of Geographical Sciences, **20**(4), 599–612.
468   Zarghami, M., Abdi, A., Babaeian, I., Hassanzadeh, Y., and Kanani, R. (2011) Impacts of climate change on
469   runoffs in East Azerbaijan, Iran. Global and Planetary Change, **78**(3), 137–146.
470   Zhang, P., Deng, X., Long, A., Xu, H., Ye, M., and Li, J. (2019) Change in Spatial Distribution Patterns and
471   Regeneration of Populus euphratica under Different Surface Soil Salinity Conditions. Scientific Reports, **9**,
472   9123.
473   Zhang, X. (2010) Zhang, X. Runoff change and its response to climate change in Aksu River Basin.
474   Zhou, T., Wu, P., Sun, S., Li, X., Wang, Y., and Luan, X. (2017) Impact of Future Climate Change on
475   Regional Crop Water Requirement—A Case Study of Hetao Irrigation District, China. Water, **9**(6), 429.
476   Zhu, B., Xue, L., Wei, G., Zhang, L., and Chen, X. (2019) CMIP5 projected changes in temperature and
477   precipitation in arid and humid basins. Theoretical and Applied Climatology, **136** (3), 1133–1144.
478   Zou, M., Kang, S., Niu, J., and Lu, H. (2020) Untangling the effects of future climate change and human
479   activity on evapotranspiration in the Heihe agricultural region, Northwest China. Journal of Hydrology, **585**,
480   124323.

Figure 1

Location of study area.
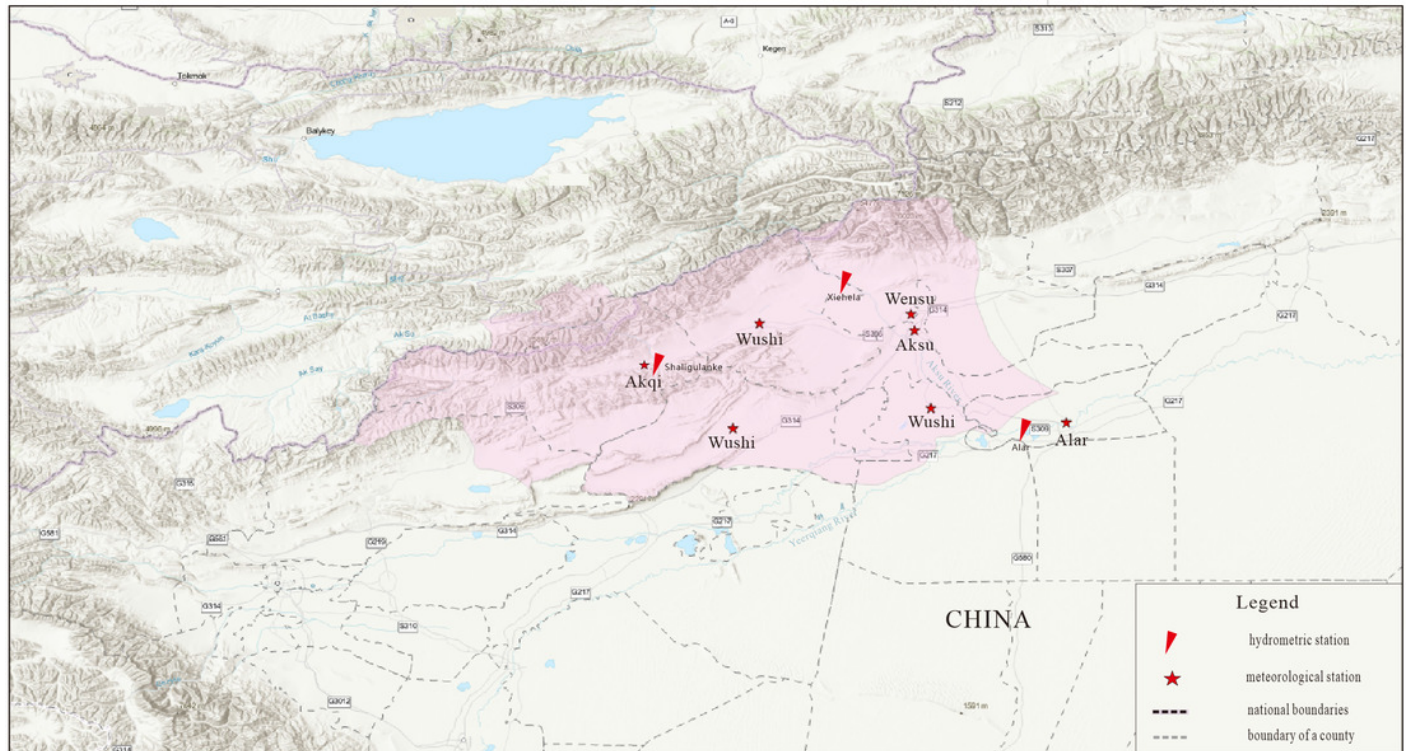
Figure 2

Flowchart for the MOGWO algorithm

```
                         ┌──────────────┐
                         │    Begin     │
                         └──────────────┘
                                │
                                ▼
        ┌───────────────────────────────────────────────────┐
        │ Identify The Gray Wolf population;maximum iterations;Archive │
        │   population size;The range of fitness function     │
        └───────────────────────────────────────────────────┘
                                │
                                ▼
              ┌───────────────────────────────────┐
              │   Initialize the Gray Wolf population │
              └───────────────────────────────────┘
                                │
                                ▼
              ┌───────────────────────────────────┐
              │     Initialize parameter i a; A; C  │
              └───────────────────────────────────┘
                                │
                                ▼
        ┌───────────────────────────────────────────────────┐
        │ Calculate all fitness function values of the initial wolves, judge │
        │ the dominant relationship, and store all non-dominant solutions │
        │        that meet the value range into Archive       │
        └───────────────────────────────────────────────────┘
                                │
                                ▼
              ┌───────────────────────────────────┐
              │       Updated parameter a; A; C     │
              └───────────────────────────────────┘
                                │
                                ▼
        ┌───────────────────────────────────────────────────┐
        │    Play roulette and choose the lead Wolf from Archive │
        └───────────────────────────────────────────────────┘
                                │
                                ▼
        ┌───────────────────────────────────────────────────┐
        │ Calculate the position under wolves and its corresponding fitness function │
        └───────────────────────────────────────────────────┘
                                │
                                ▼
        ┌───────────────────────────────────────────────────┐
        │ Compare the dominant relationship between all function values and the │
        │ Achieve set solution and store the non-dominant solution to the Archive │
        └───────────────────────────────────────────────────┘
                                │
                                ▼
                    ◇ Whether the population size ◇ ──No──┐
                                │                          ▼
                               Yes        ┌────────────────────────────────┐
                                │         │ Eliminate the solution of the   │
                                │         │ crowded area until the upper limit │
                                │         │  of population is met            │
                                │         └────────────────────────────────┘
                                ▼                          │
    No ──── ◇ Whether the number of iterations is upper limit ◇ ◄──┘
                                │
                               Yes
                                ▼
                         ┌──────────────┐
                         │     End      │
                         └──────────────┘
```

Figure 3

Average changes of temperature (T) and rainfall (R) of the basin under RCP4.5 and RCP8.5 scenarios during 2006–2050: (A) RCP4.5; (B) RCP8.5.
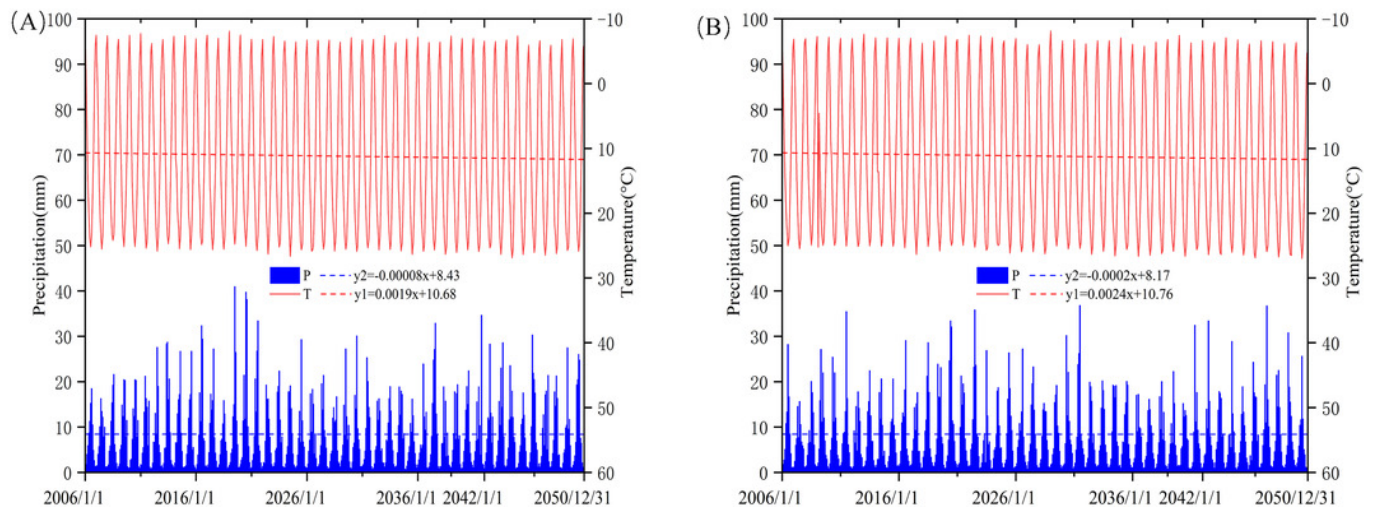
Figure 4

Average changes of reference evapotranspiration (ET0) of the basin under RCP4.5 and RCP8.5 scenarios during 2006–2050: (A) RCP4.5; (B) RCP8.5.
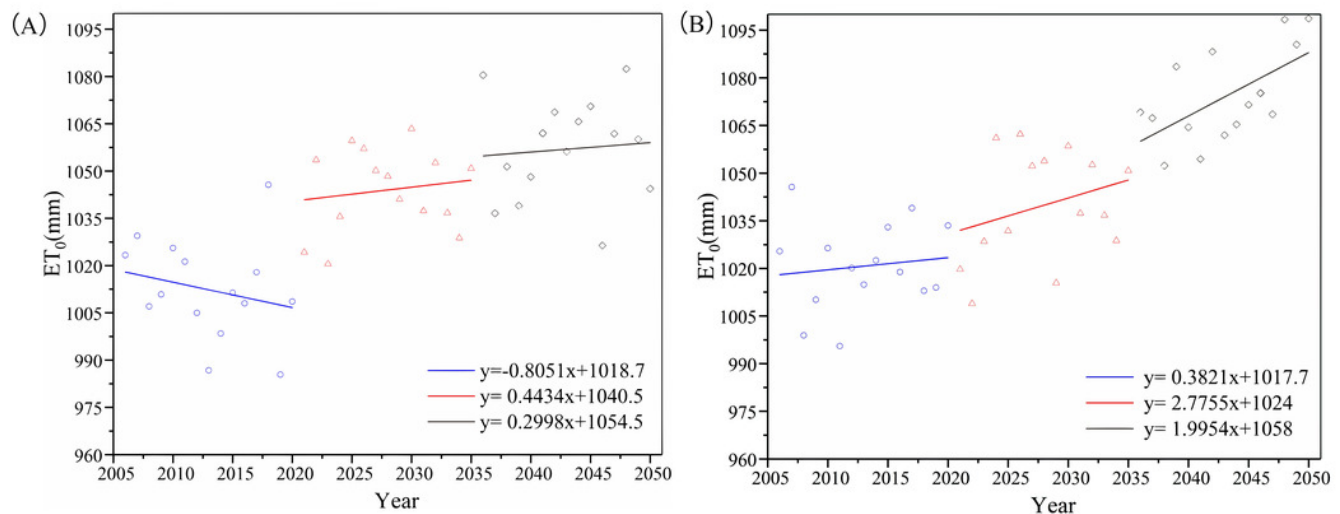
Figure 5

Average changes of reference evapotranspiration (ET_0) of the basin under RCP4.5 and RCP8.5 scenarios during 2006–2050: (A–D) Aksu, Keping, Alar, and Akqi, respectively.
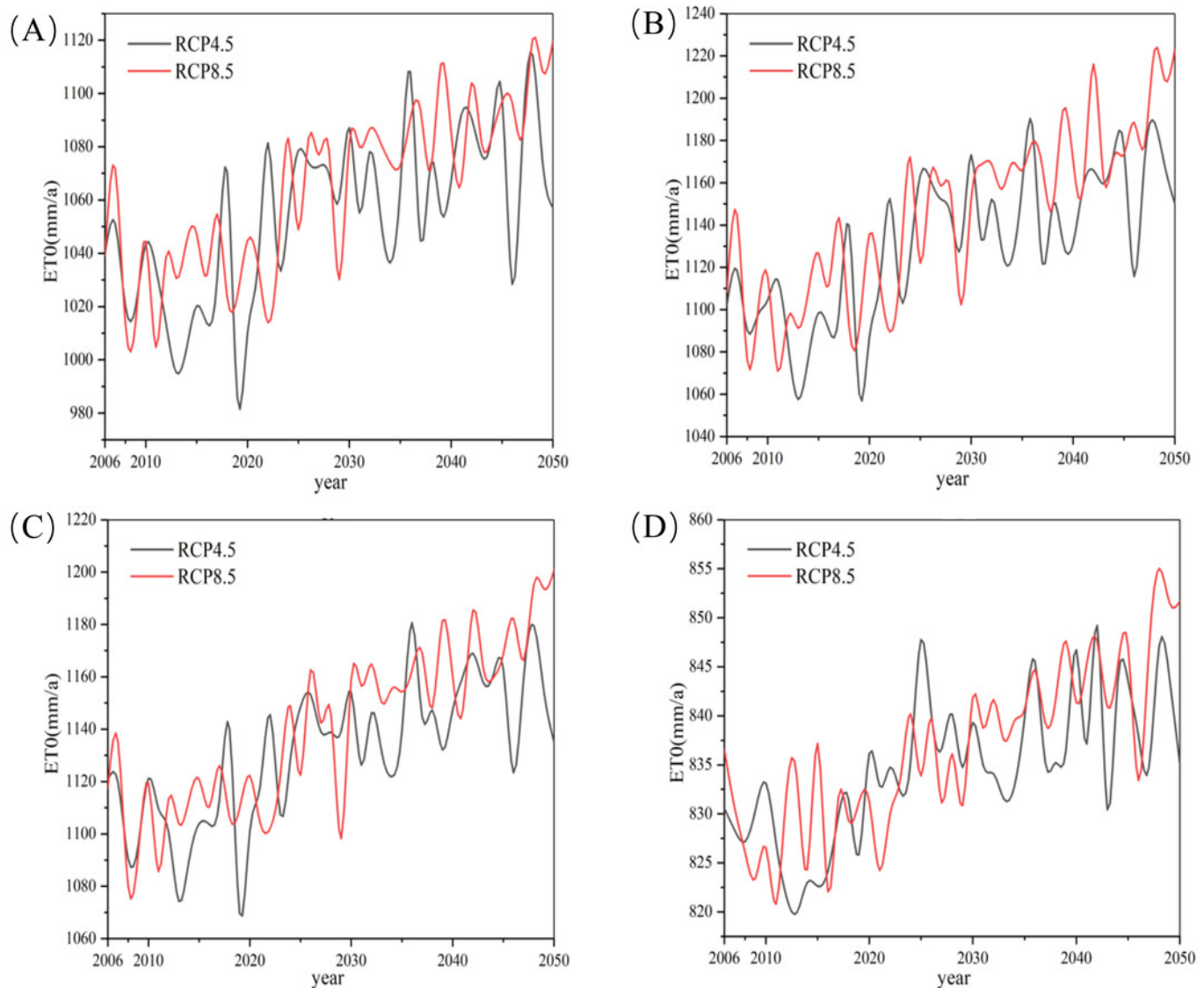
Figure 6

Neural network predictions of runoff: (A) RCP4.5; (B) RCP8.5.
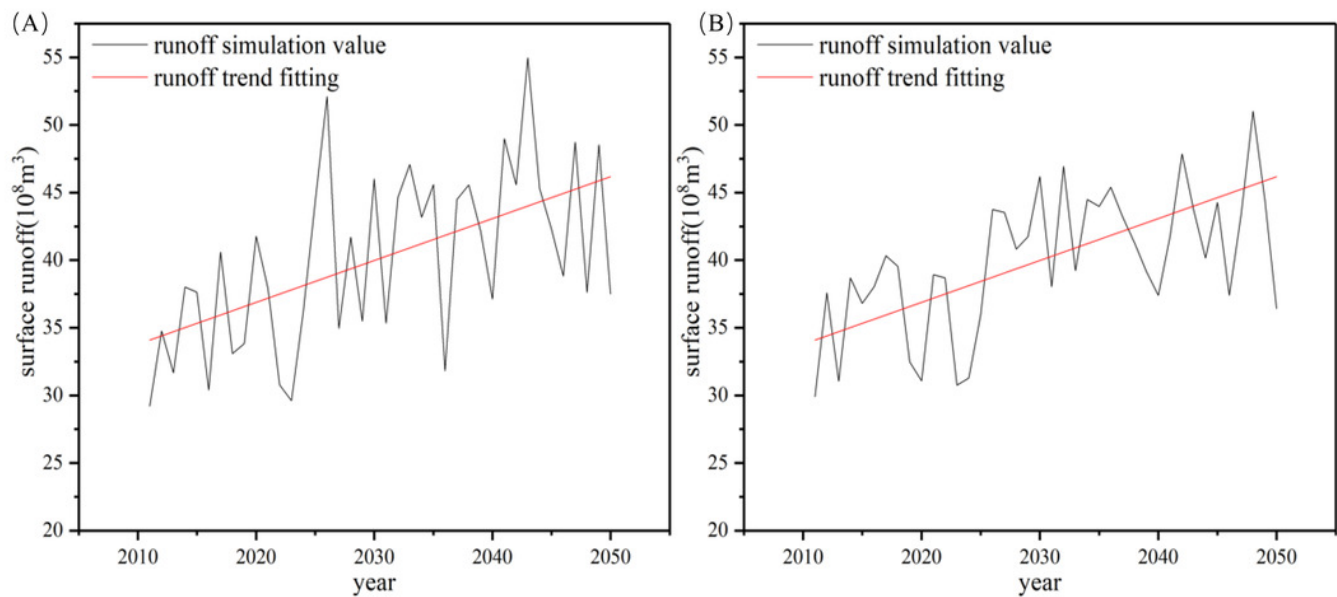
Figure 7

Allocation of water and soil resources throughout the basin: (A) RCP4.5 land resources; (B) RCP8.5 land resources; (C) RCP4.5 water resources; (D) RCP8.5 water resources. PL, plowland; GL, grassland; FL, forest land; WA, water area.
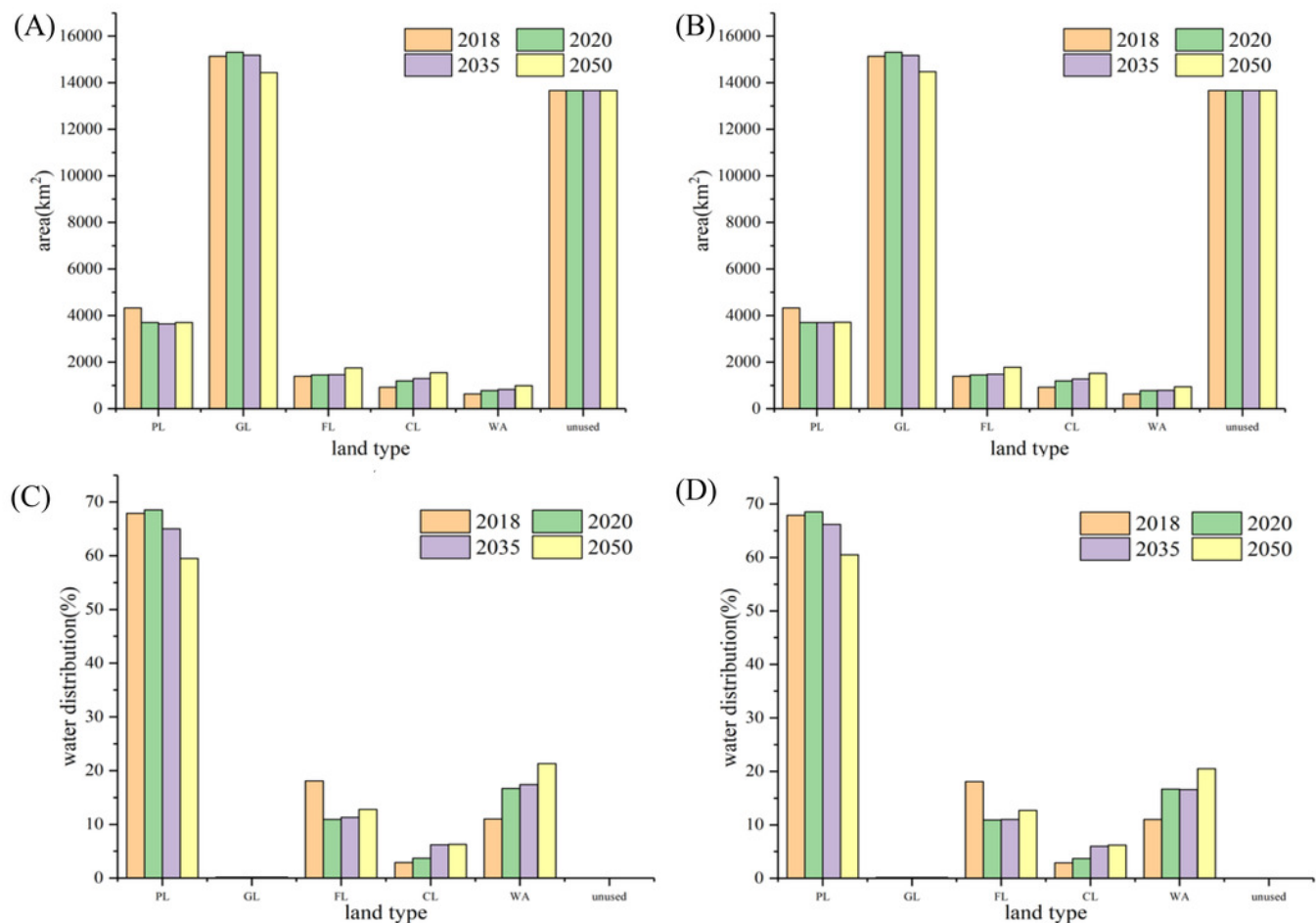
Figure 8

Allocation of plowland in each county in the basin under RCP4.5 and RCP8.5
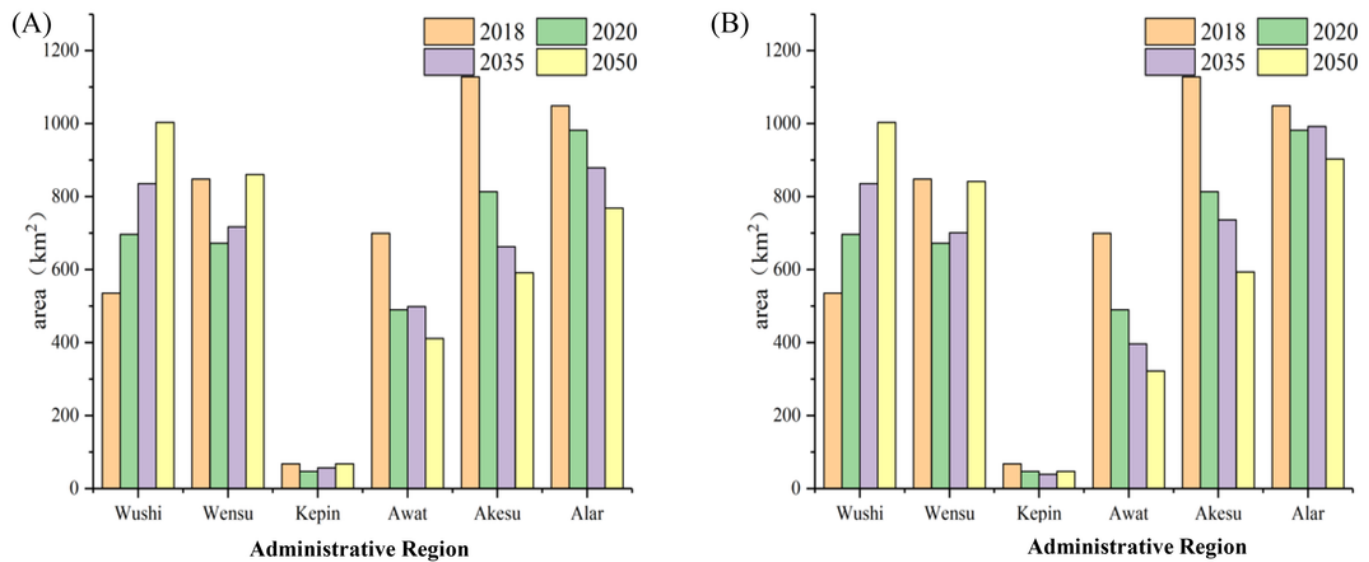
Figure 9

Allocation of grassland in each county in the basin under RCP4.5 and RCP8.5.
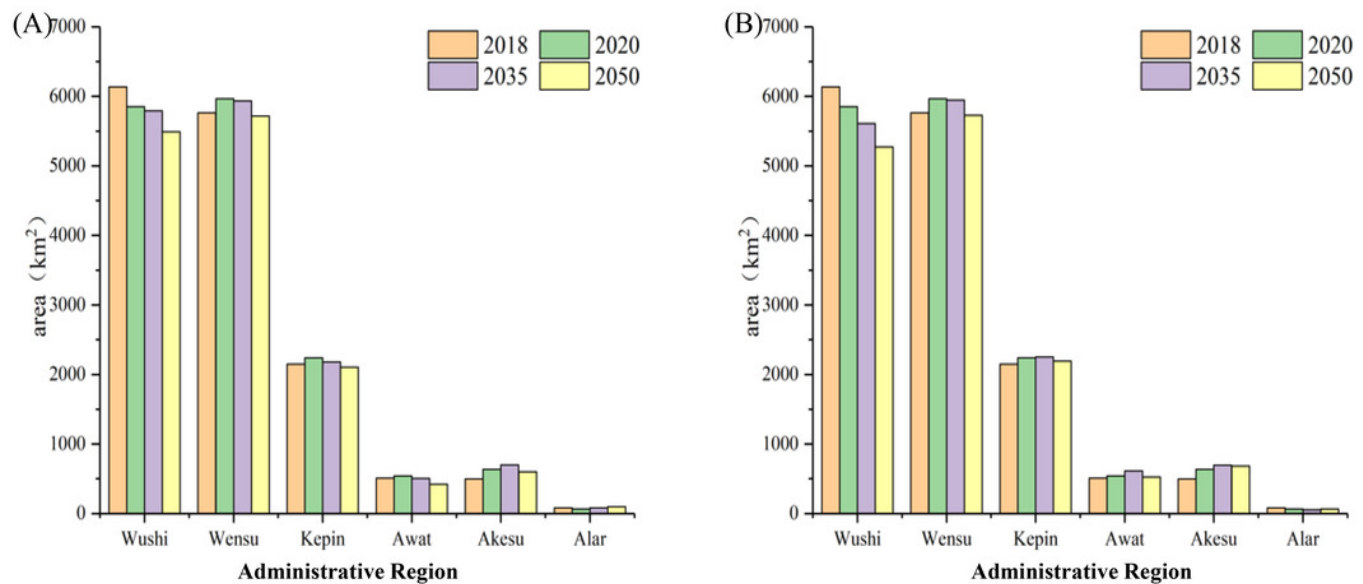
Water demand for construction land per unit area (10^4 m^3/km^2)

Administrative regions	Wushi	Wensu	Keping	Awati	Aksu	Alar
2020	11.88	23.20	16.48	6.14	17.40	10.45
2035	16.45	30.84	25.13	9.45	29.20	23.57
2050	22.11	25.31	21.19	8.50	23.81	18.18

Pairwise comparison scale for analytic hierarchy process (AHP) preferences

Definition	Equallyimportant	Moderately important	Strongly important	Verystrongimportant	Extremely important
Numerical	1	3	5	7	9

AHP calculation results.

	Weight of each target			Test rating	
	Economic benefit	Social benefit	Ecological benefit	CI	CR
2020	0.6267	0.0936	0.2797	0.0429	0.0825
2035	0.5695	0.0974	0.3331	0.0123	0.0236
2050	0.5273	0.0992	0.3735	0.0018	0.0036

Prediction results of basin water resource availability

Climate scenarios		RCP4.5			RCP8.5	
Year	2020	2035	2050	2035	2050
Available amount of water resources(10^8m^3)	47.20	50.48	51.17	52.36	53.61

Optimal solution objective function value and water resource supply and demand in RCP4.5 and RCP8.5.

		Economic benefit, GDP (10^8 yuan)	Social benefit, unilateral water benefit (yuan/m^3)	Ecological benefit, green equivalent (km^2)	Water demand 10^8m^3	Available water 10^8m^3
2018	Actual	544.21	10.47	8991.40	51.87	46.04
2020	Recent	613.53	13.00	9011.21	47.19	47.20
2035	RCP4.5	1833.82	36.33	8999.27	50.47	50.48
	RCP8.5	1836.32	35.89	9004.21	51.17	51.17
2050	RCP4.5	4909.23	97.47	9164.84	50.37	52.36
	RCP8.5	4910.22	96.93	9168.69	50.66	53.61